Check for updates

View Article Online
View Journal

RSC
Applied Interfaces

Accepted Manuscript

This article can be cited before page numbers have been issued, to do this please use: S. Misra, S. Shyam and S. K. Mitra, *RSC Appl. Interfaces*, 2026, DOI: 10.1039/D6LF00001K.

This is an Accepted Manuscript, which has been through the Royal Society of Chemistry peer review process and has been accepted for publication.

Accepted Manuscripts are published online shortly after acceptance, before technical editing, formatting and proof reading. Using this free service, authors can make their results available to the community, in citable form, before we publish the edited article. We will replace this Accepted Manuscript with the edited and formatted Advance Article as soon as it is available.

You can find more information about Accepted Manuscripts in the Information for Authors.

Please note that technical editing may introduce minor changes to the text and/or graphics, which may alter content. The journal's standard Terms & Conditions and the Ethical guidelines still apply. In no event shall the Royal Society of Chemistry be held responsible for any errors or omissions in this Accepted Manuscript or any consequences arising from the use of any information it contains.

ROYAL SOCIETY OF CHEMISTRY

rsc.li/RSCApplInter

Please do not adjust margins

View Article Online
DOI: 10.1039/D6LF00001K

ARTICLE

Trade-offs in Dual-Layer Surface Disinfection: Ozone Treatment on Surface-Immobilized Quaternary Ammonium Coatings

Received 00th January 20xx,
Accepted 00th January 20xx

DOI: 10.1039/x0xx00000x

Sirshendu Misra[†a], Sudip Shyam[†a], Sushanta K. Mitra*[a]

The COVID-19 pandemic has highlighted the importance of effective surface disinfection strategies, as contaminated droplets settling on high-touch surfaces remain a major source of pathogen transmission. While antimicrobial surface coatings such as silane-functionalized quaternary ammonium compounds (silane-quats) offer durable, contact-based protection against oncoming pathogens, their mode of action is inherently slow. Dual-action/hybrid approaches combining fast-acting oxidizing agents, such as ozone, with these antimicrobial coatings are often proposed. Previous reports have shown that ozone can act synergistically with quaternary ammonium surfactants in solution, improving short-term microbial inactivation. However, little is known about the effect of ozone on surface-bound silane-quats, where direct chemical interactions may alter long-term performance. In this study, we examine the impact of ozone exposure (in the form of aqueous suspension of ozonized micro/nanobubbles) on silane-quat-coated surfaces using bacteria-laden droplets as a model contamination scenario. We observe that ozone treatment reduces droplet spreading, indicative of lowered surface energy, and leads to diminished antimicrobial efficacy, as shown by reduced bacterial inactivation compared to untreated silane-quat coatings. Our results suggest that ozone exposure can lead to oxidative modification of the silane-quat coating, which can manifest as functional degradation of its antimicrobial performance. Our findings highlight an important caveat for combining disinfection strategies: while ozone provides rapid, on-demand microbial kill, it may simultaneously undermine the long-term effectiveness of silane-quat antimicrobial coatings. This underscores the need to evaluate chemical compatibility when designing hybrid approaches for reliable infection control in high-touch environments.

Keywords: silane-quats, QAC, ozone, micro/nano-bubbles, antimicrobial performance, droplet spreading, wettability, surface chemistry

Introduction

The COVID-19 pandemic renewed global attention on infection control and the need for effective strategies to curb microbial transmission in both clinical and shared community settings. While respiratory routes dominate viral spread, surface-mediated (fomite) transmission(1) via droplets settling on high-touch surfaces, such as doorknobs, handrails, hospital trays, elevator buttons, remains a persistent concern, especially for bacteria, given their prolonged survival(2) on inanimate substrates. Such contaminated fomites act as reservoirs for viral/bacterial pathogens(2–4), enabling indirect transfer through surface-to-hand and hand-to-face contact, which necessitates the development of robust surface disinfection approaches.

Conventional disinfection relies on active interventions, such as alcohols(5), quaternary ammonium compounds (QACs)(6), chlorine-based agents(7), thermal sterilization, and UV-C irradiation(8), which are demonstrated to be effective but are transient. For example, chemical action is limited by wet contact time and volatility/degradation; UV-C sterilization requires direct exposure to UV-irradiation and suffers from safety and power requirement constraints. Further, frequent manual application is labor-intensive and costly. Overuse also poses toxicity and environmental persistence risks, with possible development of antimicrobial tolerance.

To mitigate these constraints, antimicrobial surfaces(9) have emerged: coatings functionalized with peptides(10), heavy metal ions (silver(11), copper(12)), photocatalysts (TiO_2(13)), or polymeric/immobilized biocides(14,15) that inactivate or repel microbes without repeated intervention. Among these, silane-

[a] Micro & Nano-Scale Transport Laboratory, Waterloo Institute for Nanotechnology, Department of Mechanical and Mechatronics Engineering, University of Waterloo, 200 University Ave W, Waterloo, Ontario N2L 3G1, Canada
* Email: skmitra@uwaterloo.ca
† Equal Contribution

Open Access Article. Published on 22 June 2026. Downloaded on 6/23/2026 5:03:04 AM.
This article is licensed under a Creative Commons Attribution-NonCommercial 3.0 Unported Licence.

RSC Applied Interfaces Accepted Manuscript

View Article Online
DOI: 10.1039/D5LF00001K

functionalized QACs (silane-quats) are attractive for durable, contact-active antimicrobial function. Direct incorporation of QACs into a coating may lead to rapid leaching, fast depletion of the active biocide, and consequent elevated eco-toxicity. A more robust approach is to tether the active QAC to a polymeric backbone, thereby enabling anchoring of the biocidal group onto diverse substrates. For example, silane-quats (organosilicon quaternary ammonium compounds) use a silane backbone to covalently bond to surfaces such as glass via siloxane (Si-O-Si) linkages, while the quaternary ammonium moiety disrupts microbial membranes(14) through contact-mediated action. The advantage of these coatings lies in their prolonged efficacy, substrate versatility, and compatibility with large area applications.

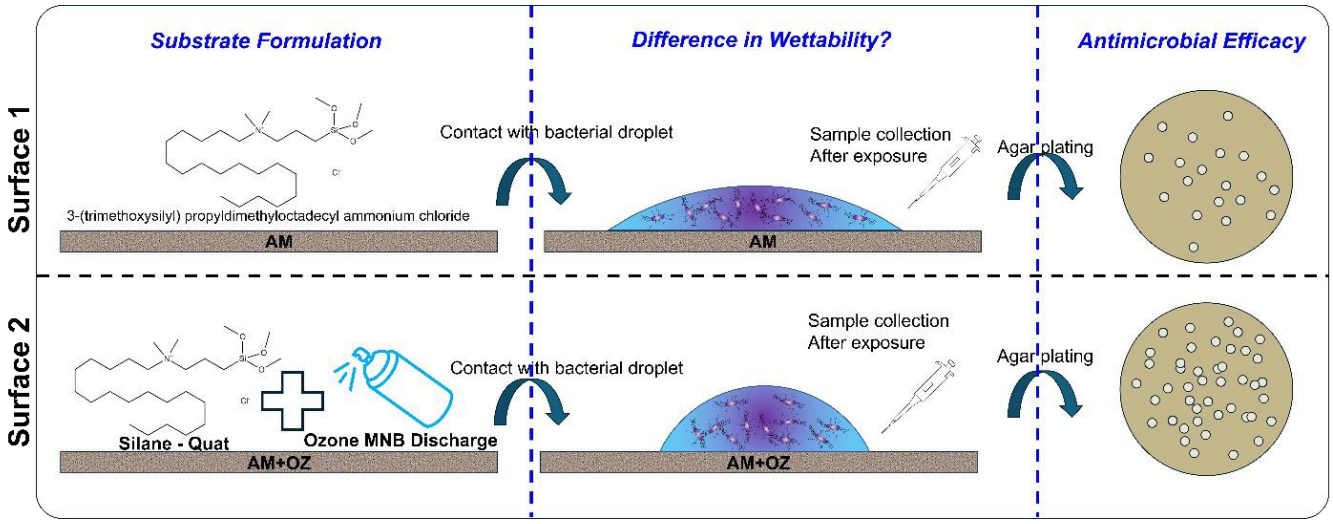

Figure 1 **Research concept: Comparative evaluation of dual-action surface disinfection.** Glass surfaces were coated with a silane-quat antimicrobial formulation (AM surfaces), with a subset of the AM-coated surfaces exposed to ozonized micro/nano-bubble discharge (AM+OZ surfaces). Wettability was evaluated using contact angle goniometry and high-speed imaging with *E. coli* test droplets, while antimicrobial efficacy was assessed by quantifying bacterial viability after surface contact.

However, a practical limitation of such surface-bound coatings is the timescale of action. While effective in reducing microbial colonization over hours to days, they may not provide immediate microbial kill, especially during the early phase of droplet deposition, where bacteria or viruses may reside within the droplet bulk(16–18) and only gradually come in contact with the surface via internal circulation and/or active motility. Notably, the interfacial interaction dynamics of droplets containing motile bacteria(16,19) or other active bioagents(20) are inherently complex compared to inert microparticles(21), with distinct physical and biological processes occurring across different timescales. In the case of passive antimicrobial surfaces, the realization of disinfection/antimicrobial action occurs over a noticeably larger timescale. Given that contaminated droplets are a primary mode of transmission in both community and clinical settings, this temporal delay presents a practical challenge for real-world application.

This motivates dual-action strategies: pairing a fast-acting oxidant (ozone, hydrogen peroxide vapor, or UV-C) for immediate/on-demand pathogen neutralization with a persistent, surface-bound biocide (e.g., silane-quats) for long-term protection. Ozone(22,23), in particular, has gained traction due to its strong oxidative potential, broad-spectrum antimicrobial activity, and ability to penetrate biofilms and porous materials. Further, it decomposes rapidly to oxygen, leaving no toxic residue, and can be easily deployed as a gas or dissolved in water for surface decontamination. In fact, some studies reported instances of synergistic improvement in disinfection capacity when ozone and quaternary ammonium surfactants are co-applied. Voumard *et al.*(24) showed that pre-exposure of *E.coli* bacteria to cetyltrimethylammonium chloride (CTMA) led to an increased susceptibility of the bacterial load to ozone disinfection, while Epelle *et al.*(25) demonstrated that ozone mist in combination with quaternary ammonium surfactants such as dodecyl trimethyl ammonium bromide (DTAB) achieved considerably higher antibacterial efficacy than either treatment alone.

Although the previous studies(24,25) indicate that combining ozone and QAC can deliver immediate/one-time benefit in antimicrobial performance, they do not take into account what happens to the QAC biocide upon ozone exposure, a crucial issue for surface-bound systems. The strong oxidative nature of ozone, while beneficial for immediate microbial inactivation, may also induce chemical transformations (oxidative degradation) in surface-bound agents. Notably, QAC ozonation and oxidative transformation(26) pathways have been documented in aqueous context. Such degradation could potentially compromise the long-term biocidal performance of otherwise effective silane-quat coatings. The key concern here, therefore, is not the short-term enhancement but the potential long-term aggravating effect on the performance of the coating. This raises a fundamental question: *does the addition of a potent oxidizing agent like ozone truly augment the antimicrobial efficacy of a pre-functionalized surface in a broader sense, or can it actually contribute to the reduction of its efficacy?*

Open Access Article. Published on 22 June 2026. Downloaded on 6/23/2026 5:03:04 AM.
This article is licensed under a Creative Commons Attribution-NonCommercial 3.0 Unported Licence.

RSC Applied Interfaces Accepted Manuscript

This journal is © The Royal Society of Chemistry 20xx

View Article Online
DOI: 10.1039/D6LF00001K

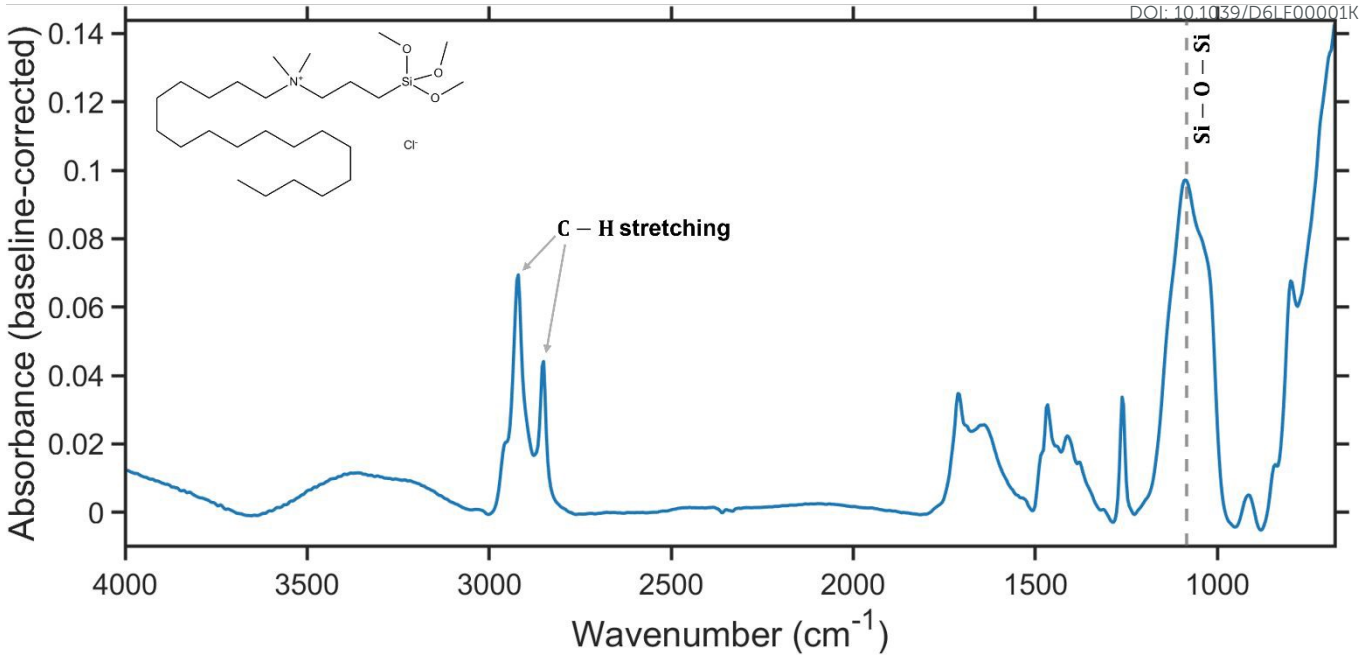

Figure 2 **Representative ATR-FTIR spectrum of the silane-quat antimicrobial coating (AM), acquired on scraped powder collected from coated glass slide.** The aliphatic $C-H$ stretching bands (~ 2920 and $\sim 2850\ cm^{-1}$), together with absorption in the $Si-O-Si$ region ($\sim 1085\ cm^{-1}$), are consistent with successful deposition of the silane coating. The inset in the top left corner shows the molecular structure of the active agent, 3-(trimethoxysilyl)propyldimethyloctadecyl ammonium chloride.

Here we evaluate whether applying ozone on silane-quat coatings, i.e., the envisioned "*dual-layer*" strategy, delivers the intended combined benefit of rapid and durable antimicrobial action or instead undermines the performance of the immobilized (surface-bound) biocide. Using a comparative framework, pristine silane-quat surfaces and ozone-treated silane-quat surfaces are assessed in terms of droplet-surface interaction and antimicrobial performance using bacteria-laden (*Escherichia coli*) test droplets. The overall research concept, including surface preparation, wettability assessment, and antimicrobial evaluation, is schematically summarized in Figure 1. Overall, our results show that ozone exposure leads to reduced droplet spreading on silane-quat surfaces and a concomitant decrease in antimicrobial efficacy relative to untreated coatings, despite negligible changes in surface morphology. These findings point to an important trade-off in dual-layer disinfection strategies, wherein rapid oxidative treatments may adversely impact the sustained performance of surface-immobilized antimicrobial coatings.

2. Materials and Methods

2.1. Preparation of Bacterial Suspension

We used *Escherichia coli* (K-12 strain SMG 123, PTA-7555, ATCC, Cedarlane, Canada) as the model microorganism. Lyophilized *E. coli* was inoculated in pre-autoclaved Lauryl Tryptose (LT) broth (Difco, DF0241170) and incubated overnight at $37°\ C$ with 100 rpm shaking to reach the stationary growth phase ($\sim 16-18\ h$). Post-incubation, $1\ mL$ of the culture was centrifuged at $10{,}000\ g$ for 10 minutes. The resulting bacterial pellet was washed twice with sterile deionized (DI) water to remove residual media and resuspended in fresh DI water. The final bacterial concentration was estimated to be $\sim 10^7\ CFU/mL$ using agar plate culturing. This suspension was used for both contact angle analysis and viability assay.

2.2. Preparation of Silane-quat Antimicrobial Surfaces

For this work, we use a proprietary antimicrobial coating formulation developed by our industry partner, SiO2 Innovation Labs, Canada. The formulation comprises a 1% quaternary ammonium silane (3-(trimethoxysilyl) propyldimethyloctadecyl ammonium chloride) in an aqueous base medium. The silane base binds to glass surfaces, while the positively charged nitrogen atom of the quaternary ammonium(14) salt attracts the negatively charged cytoplasmic membranes of the microbes. The long-chain alkyl group (chain length = 18) penetrates the membrane, leading to rapid incapacitation of the microbe.

Clean, cut glass slides ($\sim 25\ mm \times 25\ mm$) were used as base substrates. Prior to coating, the slides were ultrasonicated in acetone and subsequently rinsed in hexane, isopropanol, and deionized water, followed by drying under compressed nitrogen gas. The aforementioned silane-quat formulation ($1\ mL$) was drop-cast onto each slide and cured in an oven at 50° C for 6 hours. These substrates are referred to as AM substrates. Successful deposition of the coating was supported by Attenuated Total Reflectance-Fourier Transform Infrared (ATR-

Open Access Article. Published on 22 June 2026. Downloaded on 6/23/2026 5:03:04 AM.
This article is licensed under a Creative Commons Attribution-NonCommercial 3.0 Unported Licence.

RSC Applied Interfaces Accepted Manuscript

View Article Online DOI: 10.1039/D6LF00004K

FTIR) spectroscopy (Figure 2), which showed the characteristic aliphatic $C-H$ stretching (~ 2920, $\sim 2850\ cm^{-1}$) and $Si-O-Si$ ($\sim 1085\ cm^{-1}$) bands expected for the silane coating. Acquisition and processing details are given in Section 2.5. The inset on the top left shows the molecular structure of the active quaternary silane compound.

driven cavitation setup, which fragments the gaseous ozone phase into micro- and nanobubbles before introducing them to the continuous water stream. Once formed, these bubbles remain entrained in the flow loop. The system is equipped with a designated outlet port that allows withdrawal of ozonized water through a flow valve, while uninterrupted recirculation maintains bubble suspension and preserves ozone availability in the loop. The resulting ozonized discharge maintains an oxidation-reduction potential (ORP) > 750 mV, thus acting as a

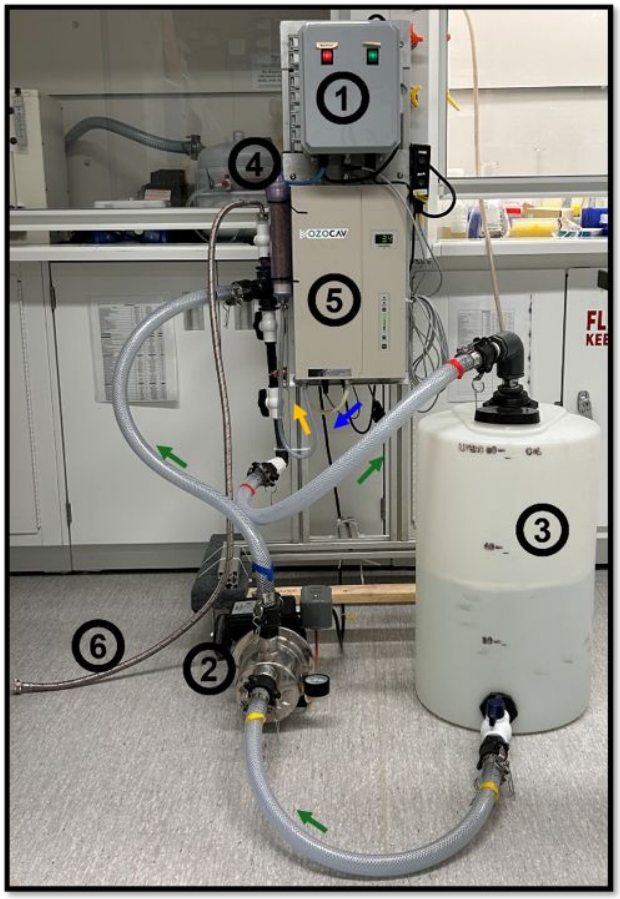

1: Power & control unit

2: Jet pump driving the water recirculation

3: Water reservoir

4: Desiccator column for removing moisture from the inlet air stream

5: Proprietary OZOCAV module responsible for corona-discharge driven O_3 generation and cavitation-driven generation of ozone micro/nanobubbles

6: Outlet connector for collecting ozonized discharge (aqueous suspension charged with ozone micro/nanobubbles)

The green arrows show the direction of water circulation, whereas the yellow and blue arrows indicate the direction of air intake into the OZOCAV module and discharge of ozonated micro/nanobubbles from the OZOCAV module, respectively.

Figure 3 **The closed-loop ozone micro/nanobubble generation setup developed by Econse Water Purification Inc.** The system integrates a jet pump, desiccant column, corona discharge-based ozone generator, and cavitation unit to produce and circulate ozonized water enriched with entrained micro/nanobubbles. An outlet port allows sample collection during continuous recirculation.

2.3. Ozonized Micro/Nanobubble Generation and Ozone Treatment

Aqueous suspensions of ozonized micro/nanobubbles were generated using a proprietary system (OZOCAV) developed by Econse Water Purification Inc. (ON, Canada). The system operates as a closed-loop recirculation unit (see Figure 3 for a visual representation of the setup) in which continuous water flow is maintained from a water tank (reservoir) using a jet pump. Ozone is generated in situ from atmospheric air via corona discharge. To improve the efficiency of ozone production, the incoming air stream is first directed through a silica-based desiccator column, which removes moisture and provides a drier feed to the corona discharge chamber. The resulting ozone stream is passed through a proprietary shear-strong oxidizer and therefore a potent antimicrobial agent.

For dual-layer treatment, $0.5\ mL$ of the aqueous suspension containing ozonized micro/nanobubbles was drop-cast onto pre-cured AM surfaces, followed by air drying for approximately 1 hour and curing in an oven at 50° C for 6 hours. These substrates are referred to as AM+OZ surfaces.

2.4. Contact Angle and Spreading Analysis

We performed contact angle measurements using a contact angle goniometer (KRÜSS DSA 30S, USA). *E. coli*-laden droplets ($\sim 3-5\ \mu L$) were used as test liquids. Separate high-speed imaging (Photron Fastcam Mini, 2000 fps) was used to capture droplet spreading (droplet volume ~4 μL) on different surfaces,

This journal is © The Royal Society of Chemistry 20xx

Open Access Article. Published on 22 June 2026. Downloaded on 6/23/2026 5:03:04 AM. This article is licensed under a Creative Commons Attribution-NonCommercial 3.0 Unported Licence.

RSC Applied Interfaces Accepted Manuscript

View Article Online
DOI: 10.1039/D6LF00001K

Open Access Article. Published on 22 June 2026. Downloaded on 6/23/2026 5:03:04 AM.
This article is licensed under a Creative Commons Attribution-NonCommercial 3.0 Unported Licence.

enabling time-resolved measurements of the spreading diameter and spreading rate.

2.5. Surface Characterization

Surface roughness characterization was performed using Atomic Force Microscopy (Nanoscope, Digital Instruments) on all surfaces. Scans were conducted in tapping mode over a $\sim 10\,\mu m \times 10\,\mu m$ area. Root-mean-square roughness (Rq) was computed for both silane-quat and ozone-treated silane-quat surfaces to assess topographical differences.

For chemical characterization, Attenuated Total Reflectance–Fourier Transform Infrared (ATR-FTIR) spectroscopy (NICOLET iN10 MX, Thermo Scientific, with a germanium ATR tip) was carried out, with particular attention to the $Si-O-Si$, $C-H$, and carbonyl regions. To avoid the spectral contribution of the underlying glass substrate (a strong $Si-O-Si$ absorber), coating material was scraped into powder form and analyzed. The $Si-O-Si$ band observed in the powder ($\sim 1085\ cm^{-1}$) therefore arises from the siloxane network of the silane coating itself, rather than from the underlying glass substrate. The same procedure was used both for confirming successful deposition (Figure 2) and for the comparative analysis of AM and AM+OZ coatings (Section 3.3, Figure 7). Spectra were collected over $4000-750\ cm^{-1}$ at $8\ cm^{-1}$ resolution, with at least three measurements acquired per condition.

Spectra were processed identically across all samples in MATLAB. Where required, transmittance was converted to absorbance, and a baseline was subtracted using an asymmetric least-squares algorithm ($\lambda = 10^5,\ p = 0.01$); the same baseline parameters were applied to every spectrum so that any difference between conditions could not arise from differential processing. To compare the extent of oxidation in a manner insensitive to sample-to-sample differences in the amount of material sampled, the degree of oxidative modification was quantified for each spectrum as the within-spectrum absorbance ratio of the carbonyl band ($\sim 1710\ cm^{-1}$) to the aliphatic C–H stretching band ($\sim 2920\ cm^{-1}$). Reported values are mean $\pm$ standard deviation across the measurements.

2.6. Antimicrobial Performance Assessment

Unless otherwise specified, the following protocol was used to assess the antimicrobial efficacy of test surfaces. A 20 µL droplet of *E. coli* base suspension was placed on each surface and left undisturbed for 10 minutes. A 10 µL aliquot was recovered from the droplet, as the complete 20 µL volume cannot be reliably aspirated from the surface due to possible evaporation and pipetting errors. The recovered 10 µL aliquot was diluted in 90 µL sterile deionized (DI) water to generate the first 10-fold dilution, followed by successive 10x serial dilutions prepared in sterile DI water. Aliquots (10 µL) from each dilution were plated on Luria-Bertani (LB) agar plates and incubated at 37°C for 18 h. Colony-forming units (CFU/mL) were enumerated and compared across untreated silane-quat (AM) substrates and ozone-treated silane-quat (AM+OZ) surfaces. All experiments were performed maintaining sterile techniques throughout.

2.7. Environmental Conditions

All experiments were conducted under controlled lab conditions ($21 \pm 1°$ C temperature, 60% relative humidity).

3. Results and Discussion:

3.1. Change in Wettability Upon Ozone Exposure

To study the effect of ozone on the silane-quat antimicrobial surface, we first evaluated the change in surface wettability. Wettability was examined by two approaches, namely, 1. monitoring the contact line behavior during dynamic spreading and 2. comparing the equilibrium droplet shape.

Dynamic spreading behavior

High-speed imaging was used to capture the spreading behavior of *E.coli* droplets (volume ~4 µL) during the first few seconds after deposition. On both surfaces, a slow, gradual spreading of the droplets was observed. Here, we do not focus on the early stage (µs-ms) spreading(27,28) behavior, but rather on spreading over several seconds to capture the overall dynamics. Accordingly, a moderate frame rate of 2000 fps was chosen during high-speed imaging.

Figure 4(a) captures the dynamic spreading behavior in terms of the temporal evolution of the contact diameter of the test droplet on both substrates. A stick-slip behavior of the contact line was observed during spreading in both cases. However, a difference in spreading rate was observed: the rate of increase in contact diameter was consistently higher on AM compared to AM+OZ. Over the ~ 6.2 s observation window, the final contact diameter reached ~ 3.8 mm on AM, whereas it was ~ 3.67 mm on AM+OZ (see the inset to Figure 4(a)). This reduction in spreading could limit the area available for contact-mediated antimicrobial action, especially in scenarios where short contact times are expected (e.g., splash or impact-driven contamination). Moreover, while the contact diameter vs. time curve for AM+OZ had nearly plateaued by the end of the observation window, the curve for AM continued to exhibit growth.

Comparison of Equilibrium Droplet Shape

RSC Applied Interfaces Accepted Manuscript

View Article Online DOI: 10.1039/D5LF00301K

Building on the observations from the dynamic spreading experiment (Figure 4(a)), we also compared the equilibrium droplet shape on both surfaces captured separately using a contact angle goniometer. Beyond the $\sim 6.2\,s$ observation window, the contact line continued to advance, particularly on AM surfaces, suggesting that even longer timescales are required to capture the stabilized droplet configuration. Accordingly, static contact angle measurements were performed once the contact line had nearly stabilized to quantify the equilibrium wetting signature.

The results are summarized in Figure 4(b). For AM, the equilibrium contact angle was measured as $13.14 \pm 2.36°$, indicating a highly wettable surface. In contrast, AM+OZ exhibited a higher equilibrium contact angle of $28.35 \pm 4.86°$, reflecting a reduction in wettability after ozone exposure. This difference is further substantiated by the contact diameter measurements: AM surfaces displayed a much larger droplet footprint (8.03 ± 0.42 mm) in equilibrium configuration compared to AM+OZ (5.67 ± 0.43 mm).

Together, these measurements indicate that exposure to aqueous discharge containing ozonated micro/nanobubbles reduces the wettability of silane-quat surfaces, as reflected by suppressed droplet spreading and higher equilibrium contact angles. The origin of this reduced wettability is examined in Section 3.3, where it is considered together with the antimicrobial performance and spectroscopic results. This reduction in wettability has important implications. Since silane-quat coatings act primarily via contact-mediated mechanisms, a smaller droplet footprint on AM+OZ limits the interfacial area available for microbial inactivation. Consequently, even if the chemical functionality were preserved, the reduced spreading itself could diminish the overall antimicrobial effectiveness of the surface under realistic scenarios involving contact with pathogen-laden droplets.

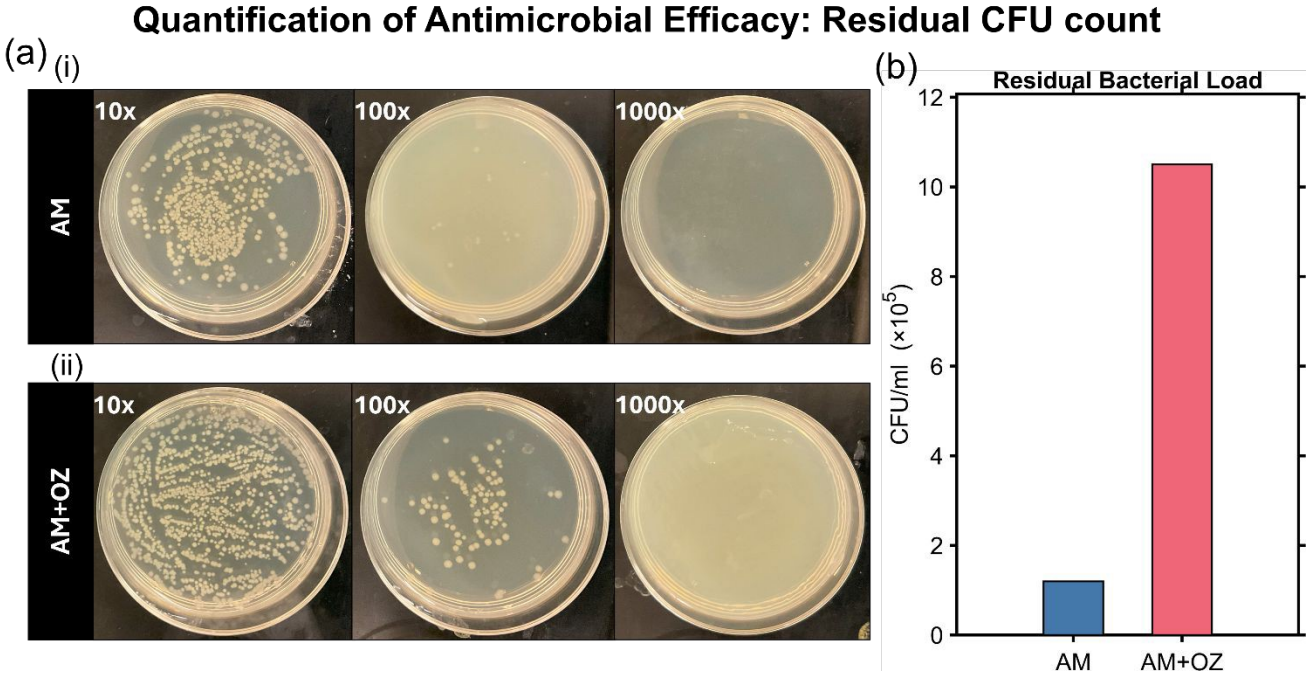

Figure 4 **Comparison of antibacterial efficacy of silane-quat surfaces before and after ozone exposure:** (a) Representative agar plate images for 10x, 100x, and 1000x dilutions of the bacterial load recovered after 10 minutes of surface contact with (i) AM and (ii) AM+OZ surfaces. (b) Bar plot comparing the residual CFU count (CFU/ml) between AM and AM+OZ, clearly showing ~10-fold lower antimicrobial activity in AM+OZ compared to AM.

3.2. Effect of Ozonation on Antimicrobial Performance

Next, the functional impact of the ozone treatment on antimicrobial efficacy was assessed by comparing the antimicrobial performance on ozone-treated and untreated silane-quat surfaces using *E.coli* as the model microbe (see **Methods** section for details on the adopted protocol for evaluating antimicrobial efficacy). In brief, surface contact was maintained between a bacterial droplet of a controlled volume and the test substrate for a predetermined time interval to allow the bacterial load to be (partially) neutralized. Thereafter, the residual bacterial load on each surface was quantified via aspiration of the bacterial droplet, subsequent serial dilution, and agar-plating, and then compared with each other (see Figure 5). The pristine silane-quat (AM) coatings demonstrated a substantial reduction in bacterial CFU, consistent with their contact-active mechanism of action. However, the ozone-treated silane-quat (AM+OZ) surfaces consistently showed noticeably higher residual CFU counts. While the residual CFU count on AM surfaces is $\sim 1.20 * 10^5$ CFU/ml, AM+OZ surfaces reported a residual CFU count $\sim 10.5 * 10^5$ CFU/ml, indicating ~10-fold higher residual viable bacterial count on AM+OZ, consistent with reduced antimicrobial performance. These results indicate that ozone exposure, when applied on silane-quat coatings, can lead to reduced antimicrobial performance under the conditions examined, despite ozone independently being an effective oxidizing disinfectant. Note that to examine

Open Access Article. Published on 22 June 2026. Downloaded on 6/23/2026 5:03:04 AM. This article is licensed under a Creative Commons Attribution-NonCommercial 3.0 Unported Licence.

RSC Applied Interfaces Accepted Manuscript

This journal is © The Royal Society of Chemistry 20xx

View Article Online
DOI: 10.1039/D6LF00001K

the effect of contact time on the comparative antimicrobial performance of the two coatings, we performed an additional assay using a shorter exposure time of 5 min. The same qualitative trend was reproduced, with AM showing lower recoverable CFU than AM+OZ (Figure S1, Supporting Information).

It is important to note that the CFU values reported here correspond to the viable bacterial population recoverable from the bulk of the droplet (i.e., the bacterial population in the planktonic state within the droplet) after the prescribed surface contact duration. Therefore, the present assay does not independently quantify bacteria that may remain adhered to the surface. A lower recoverable CFU in the bulk phase may arise either because more bacteria are inactivated due to the antimicrobial action of the surface, or because a larger fraction remains adhered to the surface and is therefore unrecoverable during sampling from the bulk liquid phase of the droplet. However, for a contact-active coating such as silane-quat, bacteria that remain adhered to the surface are also the ones expected to be exposed to the surface-attached active groups and therefore are more likely to undergo inactivation. In that sense, lower recoverable CFU still unambiguously represents a functionally favorable outcome in terms of antimicrobial efficacy. In other words, despite being unable to differentiate between planktonic and surface-adherent populations, recoverable CFU from the droplet still serves as a reliable metric to quantify antimicrobial performance.

Of course, direct visualization of surface-associated bacterial populations using microscopy-based approaches such as confocal laser scanning microscopy (CLSM), together with suitable live/dead staining, could provide additional mechanistic insight into bacterial adhesion, surface retention, and subsequent inactivation. In this context, Recupido *et al.(29)* showed that an inverted confocal microscopy framework can be used to monitor time-resolved bacterial behavior within evaporating droplets and distinguish live and dead cells over time. Additionally, in a recent study(19), we used micro-particle image velocimetry ($\mu - \mathrm{PIV}$) to probe bacterial motion and flow fields near interfaces within droplets. While that study did not directly examine surface colonization or biofilm formation, a similar bottom-view imaging approach can be extended to probe the surface interaction of bacterial populations in the present system, especially because the coatings used in the present work are optically transparent. However, incorporating such analysis would shift the focus of the present work toward detailed bacteria-surface interaction dynamics and adhesion kinetics. The present study is instead focused on examining the effect of combining multiple disinfection strategies on the overall antimicrobial performance over a relatively short interaction timespan (~10 minutes). In this context, the recoverable CFU measurements, as performed here, provide a simpler yet reliable alternative without requiring complex microscopic visualization and analysis. Direct microscopy-based examination of surface-associated bacterial populations, however, remains an interesting and relevant direction for future work.

3.3. Origin of the Observed Differences: Morphological or Functional?

To determine whether the observed changes in wetting and antimicrobial behavior could be attributed to alterations in surface morphology/roughness, Atomic Force Microscopy (AFM) was performed on both untreated (AM) and ozone-exposed silane-quat (AM+OZ) surfaces at several test locations. Representative 2D height maps and corresponding 3D topographic views are shown in Figure 6a (i, ii) for AM and Figure 6b (i, ii) for AM+OZ, respectively. AFM surface scan revealed that the RMS roughness (Rq) of both surface types remained in the range of ~38-40 nm, with no appreciable change due to ozone treatment.

This observation suggests that morphological changes are unlikely to be the dominant factor contributing to the altered spreading dynamics and antimicrobial behavior, as AFM scans performed at multiple representative locations showed no appreciable variation. These results instead point toward the possibility that ozone affects the chemical and functional integrity of the silane-quat layer.

Open Access Article. Published on 22 June 2026. Downloaded on 6/23/2026 5:03:04 AM.
This article is licensed under a Creative Commons Attribution-NonCommercial 3.0 Unported Licence.

RSC Applied Interfaces Accepted Manuscript

View Article Online
DOI: 10.1039/D6LF00001K

Open Access Article. Published on 22 June 2026. Downloaded on 6/23/2026 5:03:04 AM.
This article is licensed under a Creative Commons Attribution-NonCommercial 3.0 Unported Licence.

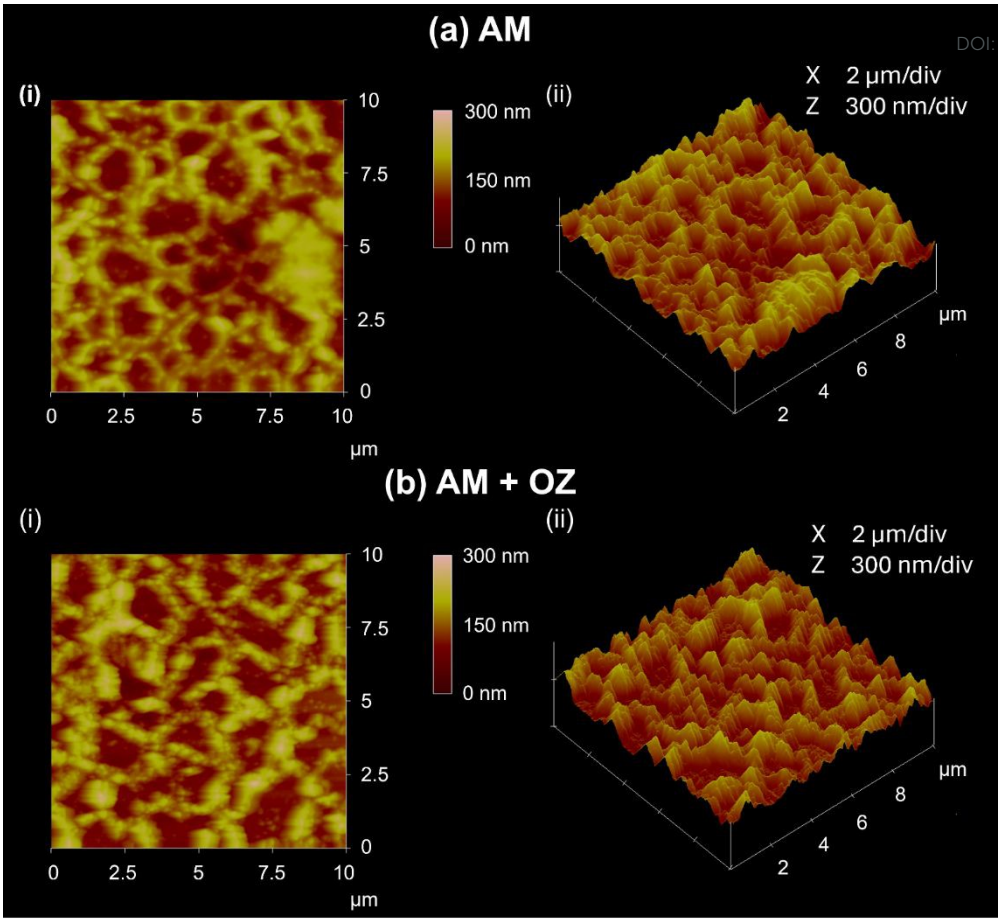

Figure 5 **AFM topographical characterization of AM and AM+OZ surfaces:** Representative (i) 2D AFM height maps and (ii) corresponding 3D topographic views of (a) untreated silane-quat coating (AM) and (b) silane-quat coating exposed to aqueous discharge containing ozonated micro/nanobubbles (AM+OZ). All scans were acquired over $\sim 10\ \mu m \times 10\ \mu m$ areas.

To examine whether ozone exposure chemically alters the coating, ATR-FTIR spectra were acquired on scraped powder from AM and AM+OZ coatings and compared (Figure 7). Two systematic changes were observed upon ozonation. First, the carbonyl region ($\sim 1710\ cm^{-1}$) showed a pronounced increase in absorbance on AM+OZ relative to AM, indicating the formation of carbonyl-containing oxidation products. Second, the aliphatic $C-H$ stretching bands (~ 2920 and $\sim 2850\ cm^{-1}$) decreased on AM+OZ, consistent with loss or fragmentation of the long alkyl chains. The siloxane backbone ($Si-O-Si$, $\sim 1085\ cm^{-1}$) was comparatively unchanged, indicating that the inorganic network remained largely intact. The spectra are shown without normalization. Minor spectrum-to-spectrum variation in the absolute intensity of the $Si-O-Si$ band is attributable to differences in the amount of powder sampled and its contact with the ATR crystal, rather than to any chemical change in the siloxane network. For this reason, the extent of oxidation was quantified using the within-spectrum carbonyl ($\sim 1710\ cm^{-1}$) to $C-H$ ($\sim 2920\ cm^{-1}$) absorbance ratio (Section 2.5), which renders the comparison insensitive to such sampling differences. Averaged over at least three measurement locations per condition, this ratio increased from 0.52 ± 0.03 on AM to 1.14 ± 0.087 on AM+OZ (mean $\pm$ standard deviation), corresponding to a roughly two-fold rise in carbonyl signal relative to the aliphatic C–H signal. Taken together, the concurrent rise in carbonyl absorbance and loss of aliphatic C–H intensity provides chemical evidence that ozone exposure oxidatively modifies the silane-quat coating, predominantly within its organic region. Note that in an early study of how ozone reacts with quaternary ammonium compounds in water, Corless *et al.*(26) examined a mixture of saturated and unsaturated quaternary ammonium surfactants and found that ozone reacted only with the unsaturated compounds, through attack at their carbon-carbon double bonds, while the fully saturated compounds were essentially unreactive. As the silane-quat used here is saturated, it would likewise be expected to resist direct molecular ozone attack. The oxidation evident in our spectra therefore points to a different, less selective oxidation route, plausibly involving reactive oxygen species generated by the ozonized micro/nanobubble system, which are capable of abstracting hydrogen from saturated $C-H$ bonds. However, we should also note that ATR-FTIR is inherently insensitive to the quaternary nitrogen centre itself. The quaternary ammonium group lacks a strong, isolated infrared signature, and its associated $C-N$ modes overlap the dominant $Si-O-Si$ envelope. Consequently, while the present spectra establish oxidation of the organic region, they cannot directly confirm or

RSC Applied Interfaces Accepted Manuscript

 This journal is © The Royal Society of Chemistry 20xx

View Article Online
DOI: 10.1039/D6LF00004K

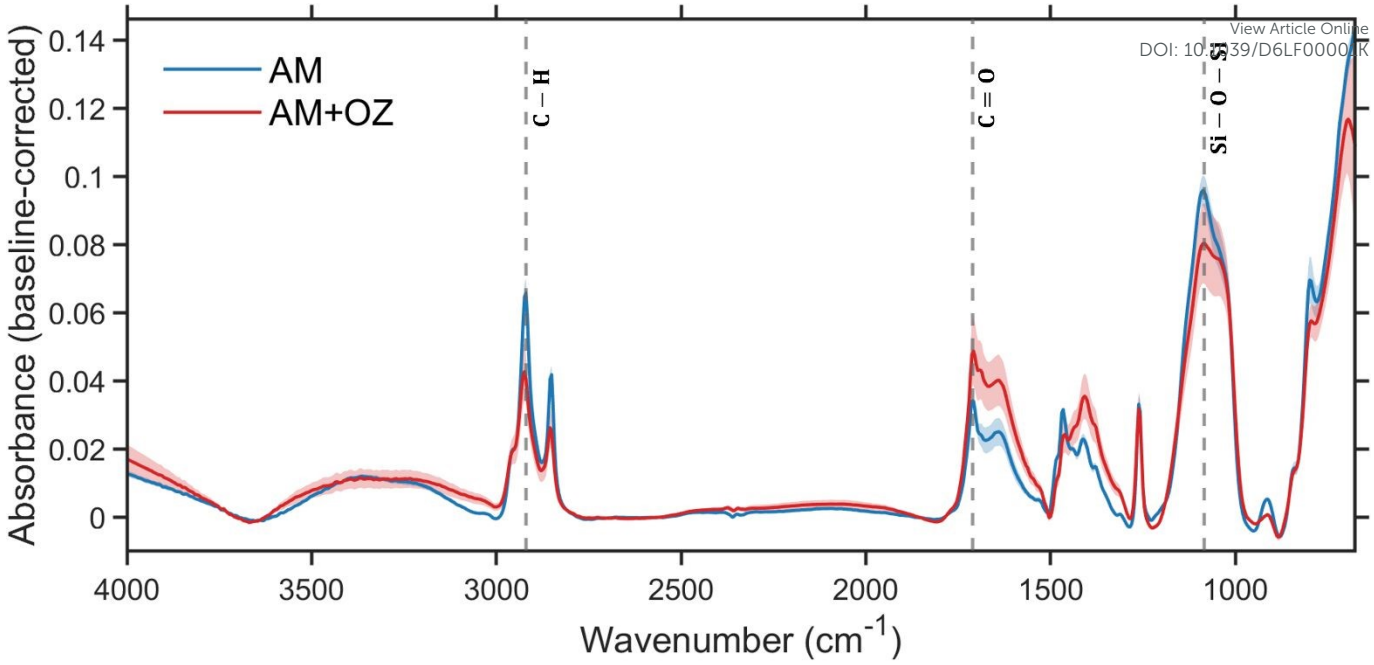

Figure 7. **ATR-FTIR spectra of untreated (AM) and ozone-treated (AM+OZ) silane-quat coatings, acquired on scraped powder and baseline-corrected.** Curves show the group mean of at least three measurements per condition; shaded bands denote ± one standard deviation. Ozone exposure resulted in a noticeable increase in absorbance in the carbonyl region near ~1710 cm^{-1} and a concurrent decrease in the aliphatic C — H stretching bands near ~2920 and ~2850 cm^{-1}. Spectra are shown without normalization; the extent of oxidation was quantified using the within-spectrum carbonyl-to-C — H ratio (see text).

exclude chemical modification at the quaternary ammonium headgroup.

This distinction is functionally important, because contact-mediated antimicrobial action depends on both the cationic headgroup and the long hydrophobic alkyl chain. The FTIR and wettability results, when considered together, provide some insight into the nature of ozone-induced modification. The FTIR spectra indicate oxidation of the organic region, with an increase in carbonyl-containing species and a concurrent decrease in aliphatic C–H intensity. Such oxidation would generally be expected to increase wettability. However, the ozone-treated surfaces (AM+OZ) instead exhibit higher contact angles and reduced spreading (Figure 4). This apparent contrast suggests that the observed wetting response is not governed solely by the organic-region oxidation detected by FTIR, but also by a concurrent reduction in the contribution of the polar, cationic headgroup, possibly through modification of the quaternary ammonium functionality and loss of its associated hydration shell. Such a change would be consistent with both the reduced wettability and the lower antimicrobial efficacy, since contact-mediated biocidal action relies also on the cationic headgroup. As noted, the quaternary nitrogen is not directly accessible by ATR-FTIR, and this interpretation remains to be confirmed by nitrogen-specific, surface-sensitive analyses such as X-ray photoelectron spectroscopy (XPS) of the N 1s region or time-of-flight secondary ion mass spectrometry (ToF-SIMS).

Conclusions

In this work, we investigated the effect of ozone exposure on silane-quat-coated surfaces by examining wettability, morphology, and antimicrobial performance. Ozone treatment led to suppressed droplet spreading, higher equilibrium contact angle, and reduced antimicrobial efficacy against *E. coli*, while AFM scans confirmed that these changes could not be attributed to a change in surface roughness. ATR-FTIR analysis showed that ozone exposure oxidatively modifies the organic region of the coating, while leaving the siloxane backbone largely intact. Furthermore, the wettability and antimicrobial efficacy results, when taken together, point toward a possible reduction in the contribution from the cationic quaternary ammonium headgroup due to ozonation. Since contact-mediated killing depends on both the organic alkyl chain and the cationic headgroup, we hypothesize that the observed oxidation of the organic region and a possible loss of the cationic headgroup contribution act together to reduce the antimicrobial effectiveness of the coating. The proposed headgroup loss would also account for the reduced wettability. In summary, the reduction in antimicrobial performance observed upon combining two disinfection methods, namely, ozone and surface-immobilized quats, underscores the importance of evaluating chemical compatibility when designing multi-layered antimicrobial strategies. While ozone alone may provide rapid microbial inactivation, its oxidative nature may degrade long-term antimicrobial coatings, especially those based on quaternary ammonium silanes.

This finding is particularly relevant in scenarios where antimicrobial surfaces are intended to retain long-term efficacy while being subjected to periodic/on-demand oxidative

Open Access Article. Published on 22 June 2026. Downloaded on 6/23/2026 5:03:04 AM.
This article is licensed under a Creative Commons Attribution-NonCommercial 3.0 Unported Licence.

RSC Applied Interfaces Accepted Manuscript

View Article Online
DOI: 10.1039/D5LA00178K

Open Access Article. Published on 22 June 2026. Downloaded on 6/23/2026 5:03:04 AM. This article is licensed under a Creative Commons Attribution-NonCommercial 3.0 Unported Licence.

cleaning. Our study suggests that such dual-action systems, if not carefully designed, may result in net performance loss rather than synergistic gain. Future efforts toward designing multilayer disinfection protocols should focus on selecting disinfection strategies that are mutually compatible/synergistic or at least non-interacting over longer timescales. Note that the wettability and functionality assessments performed in present study are restricted to freshly prepared coatings so that the immediate functional effect of ozone exposure on silane-quat antimicrobial surfaces can be isolated without additional variables associated with aging or repeated use. Coating durability after repeated/multiple ozone exposure cycles or over extended aging durations was not examined here. This remains an important practical consideration and a relevant direction for future work, which will require systematic aging and durability studies.

Conflicts of interest

There are no conflicts to declare.

Data availability

The data supporting this article have been included within the article.

Acknowledgement

The authors acknowledge the funding support from the Natural Sciences and Engineering Research Council (NSERC), Canada, in the form of the NSERC Alliance Grant Mission (ALLRP 570425-2021). The authors also thank Mathew Buchanan, SiO2 Innovation Labs, Canada, for providing them with their proprietary Protect-AM (silane-quat) formulation for preparing the antimicrobial surface coating, and Derek Davy, Econse Water Purification Inc, ON, Canada, for providing their OZOCAV unit for generating the ozonized discharge containing aqueous suspension of ozonated micro/nanobubbles. The authors also acknowledge the use of OpenAI's ChatGPT platform for proofreading and minor paraphrasing parts of the manuscript.

References

1. Otter JA, Yezli S, Salkeld JAG, French GL. Evidence that contaminated surfaces contribute to the transmission of hospital pathogens and an overview of strategies to address contaminated surfaces in hospital settings. American Journal of Infection Control. 2013 May 1;Disinfection, Sterilization and Antisepsis: Current Issues, New Research and New Technologies41(5, Supplement):S6–11. doi:10.1016/j.ajic.2012.12.004
2. Kramer A, Schwebke I, Kampf G. How long do nosocomial pathogens persist on inanimate surfaces? A systematic review. BMC Infectious Diseases. 2006 Aug 16;6(1):130. doi:10.1186/1471-2334-6-130
3. Doremalen N van, Bushmaker T, Morris DH, Holbrook MG, Gamble A, Williamson BN, et al. Aerosol and Surface Stability of SARS-CoV-2 as Compared with SARS-CoV-1. New England Journal of Medicine. 2020 Apr 16;382(16):1564–7. doi:10.1056/NEJMc2004973
4. Wißmann JE, Kirchhoff L, Brüggemann Y, Todt D, Steinmann J, Steinmann E. Persistence of Pathogens on Inanimate Surfaces: A Narrative Review. Microorganisms. 2021 Feb 9;9(2):343. doi:10.3390/microorganisms9020343 PubMed PMID: 33572303; PubMed Central PMCID: PMC7916105.
5. Ribeiro MM, Neumann VA, Padoveze MC, Graziano KU. Efficacy and effectiveness of alcohol in the disinfection of semi-critical materials: a systematic review. Rev Lat Am Enfermagem. 2015;23(4):741–52. doi:10.1590/0104-1169.0266.2611 PubMed PMID: 26444178; PubMed Central PMCID: PMC4623738.
6. Jennings MC, Minbiole KPC, Wuest WM. Quaternary Ammonium Compounds: An Antimicrobial Mainstay and Platform for Innovation to Address Bacterial Resistance. ACS Infect Dis. 2015 Jul 10;1(7):288–303. doi:10.1021/acsinfecdis.5b00047
7. Gallandat K, Kolus RC, Julian TR, Lantagne DS. A systematic review of chlorine-based surface disinfection efficacy to inform recommendations for low-resource outbreak settings. American Journal of Infection Control. 2021 Jan 1;49(1):90–103. doi:10.1016/j.ajic.2020.05.014 PubMed PMID: 32442652.
8. Demeersseman N, Saegeman V, Cossey V, Devriese H, Schuermans A. Shedding a light on ultraviolet-C technologies in the hospital environment. J Hosp Infect. 2023 Feb;132:85–92. doi:10.1016/j.jhin.2022.12.009 PubMed PMID: 36565930; PubMed Central PMCID: PMC9769028.
9. B€aumler W, Eckl D, Holzmann T, Schneider-Brachert W. Antimicrobial coatings for environmental surfaces in hospitals: a potential new pillar for prevention strategies in hygiene. CRITICAL REVIEWS IN MICROBIOLOGY. 2022;CRITICAL REVIEWS IN MICROBIOLOGY(48):531–64. doi:https://doi.org/10.1080/1040841X.2021.1991271
10. Costa F, Carvalho IF, Montelaro RC, Gomes P, Martins MCL. Covalent immobilization of antimicrobial peptides (AMPs) onto biomaterial surfaces. Acta Biomaterialia. 2011 Apr 1;7(4):1431–40. doi:10.1016/j.actbio.2010.11.005
11. Ortí-Lucas RM, Muñoz-Miguel J. Effectiveness of surface coatings containing silver ions in bacterial decontamination in a recovery unit. Antimicrob Resist Infect Control. 2017 Jun 13;6:61. doi:10.1186/s13756-017-0217-9 PubMed PMID: 28630685; PubMed Central PMCID: PMC5470207.
12. Salah I, P. Parkin I, Allan E. Copper as an antimicrobial agent: recent advances. RSC Advances. 2021;11(30):18179–86. doi:10.1039/D1RA02149D
13. Kikuchi Y, Sunada K, Iyoda T, Hashimoto K, Fujishima A. Photocatalytic bactericidal effect of TiO2 thin films: dynamic view of the active oxygen species responsible for the effect. Journal of Photochemistry and Photobiology A: Chemistry. 1997 Jun 1;106(1):51–6. doi:10.1016/S1010-6030(97)00038-5
14. Yao Y, Ye Z, Zhang Y, Wang Y, Yu C. Quaternary Ammonium Compounds and Their Composites in Antimicrobial Applications. Adv Mater Interfaces. 2024 May 1;11(17):2300946. doi:10.1002/admi.202300946
15. Bryaskova R, Philipova N, Bakov V, Georgiev N. Innovative Antibacterial Polymer Coatings. Applied Sciences. 2025 Jan;15(4):1780. doi:10.3390/app15041780
16. M KR, Misra S, Mitra SK. Microparticle Suspensions and Bacteria-Laden Droplets: Are They the Same in Terms of Wetting

RSC Applied Interfaces Accepted Manuscript

 This journal is © The Royal Society of Chemistry 20xx

View Article Online
DOI: 10.1039/D6LF00001K

Signature? Langmuir. 2021 Feb 2;37(4):1588–95. doi:10.1021/acs.langmuir.0c03365
17. Melayil KR, Mitra SK. Wetting, Adhesion, and Droplet Impact on Face Masks. Langmuir. 2021 Mar 2;37(8):2810–5. doi:10.1021/acs.langmuir.0c03556
18. Shyam S, Misra S, Mitra S, Mitra SK. Bacteria–surface interactions: role of impacting bacteria-laden droplets. Soft Matter. 2024;20(16):3425–35. doi:10.1039/D4SM00196F
19. Misra S, Shyam S, Chakraborty P, Mitra SK. Motile Bacteria-laden Droplets Exhibit Reduced Adhesion and Anomalous Wetting Behavior [Internet]. arXiv; 2025 [cited 2025 Dec 29]. Available from: http://arxiv.org/abs/2510.24535 doi:10.48550/arXiv.2510.24535
20. Shyam S, Misra S, Magdanz V, Mitra SK. Connecting Droplet Adhesion with Sperm Kinematics: A New Paradigm in Sperm Quality Monitoring. Adv Materials Inter. 2025 Jan 17;12(9):2400680. doi:10.1002/admi.202400680
21. M KR, Misra S, Mitra SK. Friction and Adhesion of Microparticle Suspensions on Repellent Surfaces. Langmuir. 2020 Nov 17;36(45):13689–97. doi:10.1021/acs.langmuir.0c02651
22. Volkoff SJ, Carlson TJ, Leik K, Smith JJ, Graves D, Dennis P, et al. Demonstrated SARS-CoV-2 Surface Disinfection Using Ozone. Ozone: Science & Engineering. 2021 Jul 4;43(4):296–305. Located at: world. doi:https://doi.org/10.1080/01919512.2020.1863770
23. Epelle EI, Macfarlane A, Cusack M, Burns A, Okolie JA, Vichare P, et al. Ozone Decontamination of Medical and Nonmedical Devices: An Assessment of Design and Implementation Considerations. Ind Eng Chem Res. 2023 Mar 15;62(10):4191–209. doi:10.1021/acs.iecr.2c03754
24. Voumard M, Breider F, von Gunten U. Effect of cetyltrimethylammonium chloride on various *Escherichia coli* strains and their inactivation kinetics by ozone and monochloramine. Water Research. 2022 Jun 1;216:118278. doi:10.1016/j.watres.2022.118278
25. Epelle EI, Cojuhari N, Mohamedsalih A, Macfarlane A, Cusack M, Burns A, et al. The synergistic antibacterial activity of ozone and surfactant mists. RSC Adv. 2023 Jul 19;13(32):22593–605. doi:10.1039/D3RA03346E
26. Corless C, Reynolds G, Graham N, Perry R, Gibson TM, Haley J. Aqueous ozonation of a quaternary ammonium surfactant. Water Research. 1989 Nov 1;23(11):1367–71. doi:10.1016/0043-1354(89)90075-4
27. Mitra S, Mitra SK. Understanding the Early Regime of Drop Spreading. Langmuir. 2016 Sep 6;32(35):8843–8. doi:10.1021/acs.langmuir.6b02189
28. Debnath D, Misra S, Kumar P, Mitra S. Understanding under-liquid drop spreading using dynamic contact angle modeling. Physics of Fluids. 2023 Oct 1;35(10):102004. doi:10.1063/5.0167659
29. Recupido F, Petala M, Caserta S, Marra D, Kostoglou M, Karapantsios TD. Forced Wetting Properties of Bacteria-Laden Droplets Experiencing Initial Evaporation. Langmuir. 2023 Jun 27;39(25):8589–602. doi:10.1021/acs.langmuir.3c00179

Open Access Article. Published on 22 June 2026. Downloaded on 6/23/2026 5:03:04 AM.
This article is licensed under a Creative Commons Attribution-NonCommercial 3.0 Unported Licence.

RSC Applied Interfaces Accepted Manuscript

View Article Online
DOI: 10.1039/D6LF00001K

Data availability

The data supporting this article have been included within the article.

Open Access Article. Published on 22 June 2026. Downloaded on 6/23/2026 5:03:04 AM.
This article is licensed under a Creative Commons Attribution-NonCommercial 3.0 Unported Licence.

RSC Applied Interfaces Accepted Manuscript